Correction procedures for extra-column effects in dynamic column breakthrough experiments

Rajendran, Arvind; Kariwala, Vinay; Farooq, Shamsuzzaman

Correction procedures for extra-column effects in dynamic column breakthrough experiments

Arvind Rajendran [a,*] Vinay Kariwala [a] Shamsuzzaman Farooq [b]

[a] *Nanyang Technological University, School of Chemical and Biomedical Engineering, 62 Nanyang Drive, Singapore 637459*

[b] *National University of Singapore, Department of Chemical and Biomolecular Engineering, 4 Engineering Drive 4, Singapore 117576*

Abstract

Dynamic column breakthrough experiments, routinely used to complement adsorption and diffusion studies at the particle scale, constitute an important step in the development and verification of dynamic models for simulation of adsorption processes. Various parts of the experimental set-up contribute to the retention time and band broadening of the experimental breakthrough curve. However, the effect of the extra-column contributions have to be properly accounted for in order to compare the experimental results with theoretical calculations. A common practice is to measure a blank response under the same flow rate, pressure and temperature conditions as the actual experiment by simply bypassing the adsorption column with a tube (or a connector) of negligible volume. This blank response is then subtracted point-by-point from the composite response (i.e., including the adsorption column) to account for extra-column contributions. The underlying assumption here is that blank and column responses are linearly additive, both in terms of mean residence time and band broadening. It is shown that this method of correction can, under certain operating conditions, lead to erroneous results. An alternative procedure based on linear regression is introduced and the improvements achieved by this method are illustrated using simulation examples.

Key words: Adsorption, Separation, Mathematical modeling, Parameter identification.

* Corresponding author.
Email address: `arvind@ntu.edu.sg` (Arvind Rajendran).

1 Introduction

Gas adsorption is an extensively used industrial separation process (Ruthven, 1984; Yang, 1987; Ruthven et al., 1994; Ruthven, 2000; Sircar, 2002). Several process configurations have been developed that skillfully exploit the adsorption thermodynamics and/or kinetics of the components involved to effect the separation. The design of these processes depend on the accuracy with which the equilibrium and kinetic parameters can be measured. Several measurement techniques, each possessing certain advantages and disadvantages, have been described in the literature (Sircar, 2007). Though static experiments, such as gravimetric and volumetric can be performed to yield accurate equilibrium and kinetic information, experiments have to be performed at process conditions; firstly to measure the performance of the column and secondly to calibrate process models that can be used for scale-up. The measurement of these parameters is often influenced by effects other than adsorption, that have to be properly accounted for. Failure to do so can lead to inaccurate estimation of equilibrium and kinetic parameters.

Dynamic column breakthrough (DCB) measurement is one of the commonly used experimental techniques and is a necessary step towards process development as it provides information about the macroscopic performance of the adsorption column. A typical DCB experiment consists of saturating the adsorption column with a gas (or gas mixture) of a known composition and switching the inlet to a gas stream that is different from the one used to saturate the column. The exit gas phase composition and flow rate is measured with suitable detectors. From this information, equilibrium and kinetic parameters can be calculated either by using analytical expressions or by fitting the experimental results to an appropriate model. It is worth noting that the "extra-column effects" or "blank contributions" arising from mechanical fittings, e.g. connecting tubing, detectors and sensors influence both the residence time and the band broadening of the breakthrough curve. Extra-column effects can be significant especially when the dead-volume in the system is not negligible. This can arise either when very short columns are used (e.g. those used for testing adsorbent materials available in small quantities) or when the residence time in the extra-column volume is non-negligible compared to the residence time in the adsorption column (Gritti et al., 2006). It is important to correct the experimentally measured breakthrough curves to eliminate these extra-column effects.

The importance of these extra-column corrections for linear chromatography has been discussed in the literature (Shankar & Lenhoff, 1991; Gritti et al., 2006). However, there has not been many investigations concerning adsorption/chromatography at non-linear conditions or when the variances of the column and the extra-column responses are not additive. Traditionally, the

correction for the extra-column effects is performed by conducting experiments where the column is replaced by a zero-dead-volume blank and subtracting this response from the composite breakthrough curve. This paper highlights the shortcomings of this correction method and proposes a model based correction procedure. Using numerical simulations to describe adsorption column dynamics, the performance of the two procedures is compared and it is shown that the new procedure accounts for the extra-column contributions with higher accuracy.

2 Modeling of adsorption column dynamics

In order to study the effect of the extra-column effects, a theoretical model is used to simulate the adsorption column. The equations used for the simulation are described below:

Mass balance for adsorbable component in gas phase:

$$\frac{\partial \overline{C}}{\partial \theta} = \frac{1}{Pe} \frac{\partial^2 \overline{C}}{\partial \chi^2} - \frac{\partial \overline{v}\overline{C}}{\partial \chi} - \psi \left(\overline{C} \frac{C_{\text{in}}}{C_{\text{T}}} - 1 \right) \frac{\partial \overline{q}}{\partial \theta} \tag{1}$$

Overall mass balance for gas phase:

$$\frac{\partial \overline{v}}{\partial \chi} = -\psi \left(\frac{C_{\text{in}}}{C_{\text{T}}} \right) \frac{\partial \overline{q}}{\partial \theta} \tag{2}$$

Mass balance for solid phase:

$$\frac{\partial \overline{q}}{\partial \theta} = \gamma \left(\overline{q}^* - \overline{q} \right) \tag{3}$$

Langmuir adsorption isotherm:

$$\overline{q}^* = \frac{\overline{C}}{1 - \lambda \left(1 - \overline{C} \right)} \tag{4}$$

Nondimensionalising scheme:

$$\overline{C} = \frac{C}{C_{\text{in}}}; \ \overline{q} = \frac{q}{q_{\text{in}}^*}; \ \chi = \frac{z}{L}; \ \overline{v} = \frac{v}{v_{\text{in}}}; \ \theta = \frac{t}{L/v_{\text{in}}}; \ C_{\text{T}} = \frac{P}{R_{\text{g}} T_{\text{in}}};$$

3

$$\psi = \frac{q_{in}^*}{C_{in}} \frac{1-\epsilon}{\epsilon}; \ \gamma = \frac{kL}{v_{in}}; \ \lambda = \frac{q_{in}^*}{q_s}; \ q_{in}^* = \frac{KC_{in}}{1+bC_{in}}; \ b = \frac{K}{q_s}; \ Pe = \frac{v_{in}L}{D_L}$$

An axially dispersed plug flow model is used to describe the mass balance of the adsorbable component. The overall mass balance accounts for axial variation of the velocity and a linear driving force (LDF) model is used to describe the solid phase mass balance. A Langmuir isotherm is used to represent the adsorption equilibrium. In the present study, the gas phase is considered to have two components: an adsorbable component and an inert carrier. The equations were discretized in space using orthogonal collocation and integrated in time using FORSIM - a stiff ordinary differential equation solver developed in Fortran (A.E. Canada, 1976).

3 Point-by-point correction

A simplified schematic of a DCB experimental set-up is shown in Fig. 1 (a). In brief, the system consists of gas tanks, a multi-position switch valve, a mass flow controller, an adsorption column, a mass flow meter, a back pressure regulator and a detector. For measuring the adsorption breakthrough curve, the column is initially saturated with an inert gas that flows through the column. At time $t = 0$, the gas flow is switched from the inert to an adsorbate of known composition. For measuring the desorption breakthrough, the procedure is reversed, i.e., the column is initially saturated with an adsorbate of known concentration and at time $t = 0$, the gas flow is switched to an inert. In both cases, the gas flow rate is controlled upstream of the column using a mass flow controller while the exit flow rate and concentration are measured using suitable detectors. It is worth noting that the sorption process can significantly affect the downstream volumetric flow rate and has to be properly accounted for to obtain reliable information (Malek et al., 1995).

Traditionally, a "point-by-point" (PBP) procedure is used to eliminate the extra-column effects and obtain the *true response* of the adsorption column (Farooq et al., 2002; Guntuka, 2006). Two sets of experiments are usually performed whose simplified schematics are shown in Fig. 1. The first experiment consists of measuring the *composite response* which represents the cumulative contribution of the extra-column volumes and the column. In the second experiment, the column is replaced by a zero-dead-volume connector whose contribution to residence time and band broadening is considered negligible and the experiment is repeated at the same inlet flow rate as the first experiment. This response termed *blank response* is shown along with the composite response in Fig. 2. In order to obtain the corrected response corresponding

4

breakthrough times for a particular gas phase concentration is considered: t_C being that of the composite response and t_B being that of the blank response. The corrected breakthrough time, t_{correc} is then calculated as:

$$t_{correc} = t_C - t_B \tag{5}$$

By performing this calculation over the entire concentration scale, the corrected breakthrough profile, as shown in Fig. 2 is obtained. This profile is *expected* to be the true response of the adsorption column to an ideal step input. The correction hinges on the assumption that the retention time and the band broadening are linearly additive and the adsorption breakthrough and the blank experiments are essentially performed at identical conditions.

4 Modeling dispersion in extra-column volume: Tanks-in-series model

The mixing in tubings and fittings, can be described in different ways with the two popular alternatives being: 1. Tanks-in-series and 2. Axial dispersion models (Levenspiel, 1998). Both are single parameter models, with the number of tanks, N, and the axial dispersion coefficient, D_L being the characteristic parameters for the two cases, respectively. The two extremes of mixing, namely plug flow and complete mixing can be described by these models through appropriate choice of these characteristic parameters.

In this work, the tanks-in-series (TIS) model is considered whose schematic is shown in Fig. 3(a). It is assumed that the lumped contribution of the tubing, detector and other fittings can be described by a system consisting of N equi-volume well mixed tanks connected in series. In essence, the response of the breakthrough apparatus can be modeled as shown in Fig. 3(b) with no distinction being made between mixing in the tubing, the detector and other fittings.

In the TIS model, the mass balance around the tank k can be represented by

$$\frac{dC_k}{dt} = \frac{Q(t)}{V_{dead}/N}\left(C_{k-1}(t) - C_k(t)\right) = \frac{1}{\tau(t)}\left(C_{k-1}(t) - C_k(t)\right); \quad k = 1, 2, \cdots, N \tag{6}$$

where V_{dead} is the total dead volume, i.e. the sum of the volumes of fittings, connecting tubing, detector, etc. and τ is the residence time in a tank. The flow rate $Q(t)$ is considered to be varying with time. The above equation has two unknown parameters, the dead volume, V_{dead} and the number of tanks,

N. The dead volume, V_{dead} can either be independently measured (e.g. by filling the tubing with a suitable liquid and measuring the volume), or can be experimentally determined (e.g. by measuring the residence time of a dilute pulse). The number of tanks, N is fitted to the experimental results to match the breakthrough profile. Note that $C_N(t)$, i.e. the outlet concentration of the Nth tank corresponds to the measured composite response $C_{\text{out}}(t)$.

In order to validate the model and to demonstrate that it can be used to describe mixing in standard breakthrough apparatus, experiments were performed using a commercial oxygen detector [Model no: Servomex 572; Servomex Limited, Sussex, England]. The details of the experimental set-up are given elsewhere (Guntuka, 2006; Guntuka et al., 2007). The experiments were conducted at flow rates lower than the recommended range in order to clearly demonstrate the contribution of the dead volume to the residence time and the band broadening. In this set-up, the detector was connected directly to the downstream of the mass flow controller. The system was flushed with nitrogen and at time $t = 0$, the flow was switched to oxygen. Experiments were conducted at two different volumetric flow rates namely 37.6 mL/min and 106 mL/min. The measured responses are shown in Fig. 4. Using the TIS model described above, both V_{dead} and N were fitted to the experimental profiles by reducing the sum of the errors between the experimental and calculated responses. The best fit was obtained for $V_{\text{dead}} = 64$ mL and $N = 11$. The corresponding calculated responses are also shown in Fig. 4. It can be seen that barring a minor mismatch in the latter part of the breakthrough curve corresponding to 106 mL/min, the fit is good. Hence, from this example, it can be argued that the TIS model offers good representation of mixing in the detector and that N can indeed be considered invariable within the range of flow rates considered (note that the two flow rates used vary by a factor of 2.8).

5   Inversion of tanks-in-series model

In the previous section, we demonstrated that the TIS model can indeed be used for the description of the dispersion in the detector. In this section, we use the TIS model for handling corrections for "extra-column" effects, i.e. estimation of the true response of the column, $C_0(t)$ from the experimentally measured composite response, $C_{\text{out}}(t)$. We first note that a rearrangment of Eqn. 6 gives

$$C_{k-1}(t) = C_k(t) + \tau(t)\frac{dC_k}{dt} \quad k = 1, 2, \cdots, N \tag{7}$$

6

The above expression suggests that $C_{N-1}(t)$ can be calculated based on the measured response $C_N(t)$ by using a finite difference approximation of the derivative term. By continuing this procedure, it may seem possible to compute $C_0(t)$ using Eqn. 7. A practical difficulty in using this approach is that the derivative term amplifies the measurement noise present in $C_N(t)$ and hence the calculated $C_0(t)$ becomes non-smooth. Furthermore, the use of finite difference approximation inherently introduces some error in the estimation of $C_{k-1}(t)$ from $C_k(t)$. Numerical examples show that even when measurement noise is not present, the error manifests itself as oscillations in the computed profiles of $C_0(t)$, especially for large N. The presence of oscillations in the computed $C_0(t)$ can also be attributed to the non-causality, i.e. the estimation of cause from effect, of the model in Eqn. 7. These difficulties necessitates the use of regression based techniques to estimate $C_0(t)$ from measured $C_N(t)$, as discussed in the rest of the section. We first deal with the case of constant volumetric flow rate at the exit of the column Q_0 (e.g. when the adsorbable component is in trace quantities) followed by the case of time-varying $Q_0(t)$.

5.1 Constant volumetric flow rate

As the composite response, $C_{\text{out}}(t)$ is only measured at finite number of time instances, we need a discretized version of the TIS model in Eqn. 6 for regression purposes. Such a discretized model can be obtained using forward or backward difference to approximate the derivative term in Eqn. 6. In this paper, we instead use Laplace transform followed by discretization using zero-order hold to get a more accurate discretized model. Specifically, the latter method ensures the response of $C_{\text{out}}(t)$ from the discretized model and differential equation model given by Eqn. 6 are the same for a step change in $C_0(t)$.

Now, denoting the deviation variables as $\widehat{C}_k(t) = C_k(t) - C_k(0)$ and using Laplace transform, the TIS model can be expressed in the transfer function form as (Seborg et al., 2003)

$$\frac{\widehat{C}_k(s)}{\widehat{C}_{k-1}(s)} = \frac{1}{\tau s + 1}; \quad k = 1, 2, \cdots, N$$
$$\Rightarrow \frac{\widehat{C}_N(s)}{\widehat{C}_0(s)} = \prod_{k=1}^{N} \frac{\widehat{C}_k(s)}{\widehat{C}_{k-1}(s)} = \frac{1}{(\tau s + 1)^N} \tag{8}$$

Based on Eqn. 8, we note that the estimation of the inlet concentration profile $C_0(t)$ through direct inversion of the TIS model is not possible as the inverse of the model between $\widehat{C}_0(s)$ and $\widehat{C}_N(s)$ is non-causal and a method for overcoming this difficulty is discussed next.

To obtain a discretized model, let Δt represent the difference between the successive time instants at which outlet concentration is recorded. For simplicity, we assume that Δt does not change during the experiment. In practice, this assumption can be satisfied in two ways: 1.) By performing data acquisition at desired time intervals or 2.) by using (nearest neighbor or spline) interpolation on the irregularly recorded outlet concentration profile. The transfer function model between $\widehat{C}_0(s)$ and $\widehat{C}_N(s)$ is discretized using zero-order hold with a sampling period Δt and g_j is taken as the jth step response coefficient of the discretized model. Then, the outlet concentration profile $\widehat{C}_N(i)$, $i = 1, 2, \cdots, n_{\text{samp}}$ can be computed using convolution as (Seborg et al., 2003)

$$\widehat{C}_N(i) = \sum_{j=1}^{i} g_j \, \Delta \widehat{C}_0(i - j + 1); \quad i = 1, 2, \cdots, n_{\text{samp}} \tag{9}$$

where $\Delta \widehat{C}_0(i - j + 1) = \widehat{C}_0(i - j + 1) - \widehat{C}_0(i - j)$ with $\Delta \widehat{C}_0(1) = 0$. For notational convenience in subsequent discussion, Eqn. 9 is represented in the matrix form as

$$\widehat{\mathbf{C}}_N = G \, \Delta \widehat{\mathbf{C}}_0 \tag{10}$$

where

$$\widehat{\mathbf{C}}_N^T = \left[\widehat{C}_N(1) \; \widehat{C}_N(2) \; \cdots \; \widehat{C}_N(n_{\text{samp}}) \right]^T$$

$$\Delta \widehat{\mathbf{C}}_0^T = \left[\Delta \widehat{C}_0(1) \; \Delta \widehat{C}_0(2) \; \cdots \; \Delta \widehat{C}_0(n_{\text{samp}}) \right]^T$$

and G is a Hankel matrix defined as

$$G = \begin{bmatrix} g_1 & 0 & 0 & \cdots & 0 \\ g_2 & g_1 & 0 & \cdots & 0 \\ g_3 & g_2 & g_1 & \cdots & 0 \\ \vdots & \vdots & \ddots & \cdots & \vdots \\ g_{n_{\text{samp}}} & g_{n_{\text{samp}}-1} & g_{n_{\text{samp}}-2} & \cdots & g_1 \end{bmatrix}$$

Let $\widehat{\mathbf{C}}_{N,m}$ denote a vector containing the measured outlet concentration profile expressed in terms of deviation variables, *i.e.*

$$\widehat{\mathbf{C}}_{N,m}^T = \left[\widehat{C}_{N,m}(1) \; \widehat{C}_{N,m}(2) \; \cdots \; \widehat{C}_{N,m}(n_{\text{samp}}) \right]^T$$

with $\widehat{C}_{N,m}(i) = C_{N,m}(i) - C_{N,m}(0)$. Here, a robust estimate of the initial steady-state value $C_{N,m}(0)$ can be obtained by taking the average of first few experimental data points.

It may seem that the inlet concentration profile can be estimated by minimizing the sum of squared errors (SSE), i.e. the difference between the measured and predicted outlet concentration profiles:

$$\min_{\Delta\widehat{\mathbf{C}}_0} \left(\widehat{\mathbf{C}}_{N,m} - G\,\Delta\widehat{\mathbf{C}}_0\right)^T \left(\widehat{\mathbf{C}}_{N,m} - G\,\Delta\widehat{\mathbf{C}}_0\right) \tag{11}$$

As G is a square matrix, the optimal solution for the optimization problem in Eqn. 11 is given as $\widehat{\mathbf{C}}_0^* = G^{-1}\widehat{\mathbf{C}}_{N,m}$. However, we recall that inverse of the TIS model is non-causal. This implies that the Hankel matrix G is non-invertible and the inlet concentration profile estimated as $G^{-1}\widehat{\mathbf{C}}_{N,m}$ will result in large variations.

These large variations in the inlet concentration profile can be avoided through regularization or Ridge regression, where the variation of inlet concentration is penalized (Tikhonov, 1963; Hoerl & Kennard, 1970). In particular, the following optimization problem is solved

$$\min_{\Delta\widehat{\mathbf{C}}_0} \left(\widehat{\mathbf{C}}_{N,m} - G\,\Delta\widehat{\mathbf{C}}_0\right)^T \left(\widehat{\mathbf{C}}_{N,m} - G\,\Delta\widehat{\mathbf{C}}_0\right) + \beta \left(\Delta\widehat{\mathbf{C}}_0^T \Delta\widehat{\mathbf{C}}_0\right) \tag{12}$$

where $\left(\Delta\widehat{\mathbf{C}}_0^T \Delta\widehat{\mathbf{C}}_0\right)$ is the norm of the input change. In Eqn. 12, the regularization or Ridge parameter $\beta > 0$ provides a trade-off between the prediction error and variation of inlet concentration profile. By finding the stationary point of the expression in Eqn. 12, the optimal solution can be derived as

$$\Delta\widehat{\mathbf{C}}_0^* = (G^T G + \beta I)^{-1} G^T \widehat{\mathbf{C}}_{N,m} \tag{13}$$

Based on Eqn. 13, the estimated inlet concentration profile is given as

$$C_0^*(i) = C_{N,m}(0) + \sum_{j=1}^{i} \Delta\widehat{C}_0^*(j); \quad i = 1, 2, \cdots, n_{\text{samp}} \tag{14}$$

Note that the initial value of C_0 is taken to be same as the initial value of measured outlet concentration. This is reasonable as the TIS model has unity gain (see Eqn. 8).

Note that as β is increased, the inlet concentration profile becomes smoother, but the prediction error increases. There are a number of methods available for

9

appropriate selection of β. In this paper, we use the L-curve method (Hansen, 1992), where the SSE $\left(\widehat{\mathbf{C}}_{N,m} - G\,\Delta\widehat{\mathbf{C}}_0^*(\beta)\right)^T \left(\widehat{\mathbf{C}}_{N,m} - G\,\Delta\widehat{\mathbf{C}}_0^*(\beta)\right)$ and inlet concentration variation $\left(\Delta\widehat{\mathbf{C}}_0^T(\beta)\Delta\widehat{\mathbf{C}}_0(\beta)\right)$ are computed for different values of β and plotted against each other. This curve has an L shape and β is selected around the corner of this curve.

5.2 Varying volumetric flowrate

Next, we propose an approach to handle the case where the volumetric flowrate Q_0 itself changes during the experiment (e.g. bulk adsorption). We consider that the effect of change in Q_0 is instantaneously reflected across all N tanks. Denoting Q_{in} as the flowrate at the column inlet, the transfer function model between $\widehat{C}_0(s)$ and $\widehat{C}_N(s)$ can be derived as

$$\frac{\widehat{C}_N(s)}{\widehat{C}_0(s)} = \frac{1}{\left(\frac{\tau}{Q_0/Q_{\mathrm{in}}}s + 1\right)^N} \tag{15}$$

As the measurement of Q_0 is only available at a finite number of points, we reasonably assume that Q_0 remains constant between two successive measurements. Then, the TIS description in Eqn. 15 can be seen as a piecewise linear model with a varying time constant. By discretizing the model with a sampling period of Δt and following the same procedure, as used for the case of constant volumetric flow rate in Section 5.1, it can be shown that the relationship in Eqn. 10 still holds, except that the Hankel matrix G needs to be modified as

$$G = \begin{bmatrix} g_1(1) & 0 & 0 & \cdots & 0 \\ g_2(2) & g_1(2) & 0 & \cdots & 0 \\ g_3(3) & g_2(3) & g_1(3) & \cdots & 0 \\ \vdots & \vdots & \ddots & \cdots & \vdots \\ g_{n_{\mathrm{samp}}}(n_{\mathrm{samp}}) & g_{n_{\mathrm{samp}}-1}(n_{\mathrm{samp}}) & g_{n_{\mathrm{samp}}-2}(n_{\mathrm{samp}}) & \cdots & g_1(n_{\mathrm{samp}}) \end{bmatrix} \tag{16}$$

where $g_j(i)$ is the jth step response coefficient of the discretized form of Eqn. 15 with $Q_0 = Q_0(i)$, $i = 1, 2, \cdots n_{\mathrm{samp}}$. With G in Eqn. 16, the optimal estimate of inlet concentration profile can be computed using Eqn. 13 and Eqn. 14. This formulation is more general and the situation when Q_0 is a constant over time is a special case.

10

The performance of the inversion procedure was tested using simulations. As a test case, a system with $N = 20$ and $V_{\text{dead}} = 60$ mL and an inlet flow rate of 60 mL/min was considered. An arbitrary breakthrough curve, i.e. the true response of an adsorption column, was considered as an input to the TIS model and by solving Eqn. 6, $C_N(t)$ was obtained. This response, equivalent to $C_{\text{out}}(t)$, was corrected for extra-column effects using the inversion procedure described above. The effect of the parameter β on the SSE is shown in Fig. 5, where the characteristic "L" shape can be observed. As discussed, $\beta = 0.1$ - a value around the corner of the curve was chosen for the inversion.

Two examples, one where the volumetric flow rate is constant over the period of the experiment and the other, where the flow rate varies with time were considered. Figure 6 (a) corresponds to a situation in which the volumetric flow rate is assumed to be constant throughout the duration of the experiment and it can be seen that the performance of the inversion procedure is good since the true and the corrected responses are identical. Figure 6 (b) corresponds to a situation where the exit volumetric flow rate varies with time as shown. Using this information the inversion was performed and the results demonstrate that the true and corrected results are indeed identical.

6   Results and discussion

In the earlier sections, it has been shown that the TIS model is well suited to describe the dynamics of extra-column volumes and that the model inversion can be achieved using regression based method. In this section the shortcomings of the PBP correction procedure is demonstrated and it is shown that the TIS model provides better correction.

For the sake of simplicity a dead volume of 60 mL is considered. With respect to the number of tanks, two cases are considered: namely $N = 5$ and $N = 20$. Note that these two cases represent situations that are both less well-mixed ($N = 20$) and more well-mixed ($N = 5$) compared to the experimental system for which $N = 11$ as discussed in Section 4.

For each example, the following three responses to a step input are simulated: 1.) Blank response ; 2.) True response; and 3.) Composite response. The blank response is simulated using the tanks in series model as represented by Eqn. 6, while the true response of the column is simulated using the equations listed in Section 2. The composite response of the system is simulated by processing the true response of the column through the tanks-in-series model. It is worth noting that we had demonstrated that the TIS model can indeed be used to describe extra-column in Section 4. Hence, it can be argued that this model adequately captures the contribution of the extra-column volume both

in terms of residence time and band broadening. Note that these simulations are designed to mimic the experimental runs, i.e. all three runs are performed at a pre-determined inlet flow rate and composition. Using these profiles, the two correction procedures, namely PBP and TIS are applied and the corrected response of the column to a step input is calculated. The profiles obtained by the two methods are then compared with the true response of the adsorption column. The parameters used for the various cases are given in Tables 1 and 2

6.1 Case 1

As a first example, we consider a trace system ($X_{in} = 0.05$) with a moderate non-linearity ($\lambda = 0.10$). The simulations and results for this case are shown in Fig. 7. Owing to the trace amount of the adsorbable component in the feed, the variation of the exit flow rate is negligible. The composite response was corrected for the effect of the blank using the PBP method and the results are compared with the true response of the column. Both the true and corrected responses are fairly symmetric about their mean residence time. While the corrected response estimates the mean residence time well, the estimation of the band broadening is rather poor. For both cases, i.e., $N = 5$ and $N = 20$, the PBP method estimates a sharper response than the true response of the column. This is a clear pitfall of the method and will lead to an overestimation of the mass transfer parameter if they are fitted to this response. As can be seen from the figure, the deviation of the corrected response from the true response is larger in the case of $N = 5$ as compared to $N = 20$. The TIS method with $\beta = 0.1$ was used to correct for the extra-column effects and results are plotted in Fig. 7. As can be seen from the figure, the match between the corrected and true response of the column is excellent.

6.2 Case 2

As a second example we consider a system which involves a trace system ($X_{in} = 0.05$) with a higher isotherm non-linearity ($\lambda = 0.5$). Further, the LDF coefficient is smaller as compared to Case 1. The results are shown in Fig. 8. This case corresponds to a situation where the variation of the exit flow rate over time is rather negligible as the inlet stream contains only 5 % of the adsorbable component. First we consider the corrected profiles using the PBP scheme. From the figures it can be seen that in both cases, i.e. $N = 5$ and $N = 20$ the corrected profile has a mean residence time identical to that of the true response of the column. However, the PBP method predicts a sharper response compared to the true response of the column. Further, it can be ob-

12

served that a sharp breakthrough at $t < 50$ s is seen in the true response. This is a signature of systems that are characterized by barrier resistance (Farooq et al., 2002) [1]. However, this characteristic take-off is conspicuously absent in the corrected profile. Similar to Case 1, the PBP corrected response approaches the true response when N increases. Hence, the PBP method not only estimates a sharper response but also masks signature features of actual mass transfer resistances such as barrier resistances confined at the mouth of a microporous adsorbent. As a next step, the TIS model was used for the correction and the profile is shown in the same plot. It can be clearly seen that this procedure captures the true response of the column perfectly. It captures the mean retention time, the band broadening and the characteristic take-off well.

6.3   Case 3

The third example considers a system where the inlet flow rate is five times that of the previous cases. Further, the amount of adsorbable components in the feed is increased to 50%. The results are shown in Fig. 9. It is worth noting that owing to significant amount of the adsorbable component in the feed, the exit flow rate change in this case is non-negligible. Under these conditions, the residence time in the column is much larger compared to the residence time in the blank. Both PBP and TIS schemes produce identical results which compare well with the true response of the column. In this case, owing to the high flow rate, the detector behaves like a plug flow system and hence its contribution to the band broadening, compared to that of the column, is negligible.

6.4   Case 4

The fourth example concerns a system with a fairly non-linear isotherm, $\lambda = 0.9$ and with the inlet mole fraction being $X_{\text{in}} = 0.5$. The results are shown in Fig. 10. The high fraction of adsorbable component leads to a significant change in the flow rate as the breakthrough proceeds. The PBP correction method not only produces a sharper response, but also results in a lower average retention time as compared to the true column response. This is especially visible in the Fig. 10 (b). This arises due to the fact that while the composite response is influenced by the change in flow rate, the detector response used in the PBP correction is measured at a constant flow rate which is equal to the column inlet flow rate. This is a key shortcoming of the PBP

---

[1] It should be mentioned that the LDF formulation is the correct model for describing systems that show barrier resistance.

method, and could be of concern especially when bulk adsorption is involved. In such cases, the PBP procedure could not only result in an error in the mass transfer parameters, but also result in the incorrect estimation of equilibrium parameters that might be fitted to these breakthrough curves. The comparison of the TIS corrected profile with the true column response is also shown in the same figure. It can be clearly seen that this procedure captures both the retention and band broadening well. This result is not surprising as the TIS model explicitly uses the information about the exit flow rate to perform the correction and hence allows for a better correction.

6.5 Case 5

As a final example we consider an extreme case where the mass transfer coefficient is fairly small $k = 0.001\mathrm{s}^{-1}$. The results for this case are shown in Fig. 11. The adsorbable component is diluted in the carrier and hence the variation in the exit flow rate is negligible. However, since the mass transfer coefficient is small, a very sharp breakthrough followed by a long tail is observed. The profile obtained using the PBP method is shown alongside. As in the previous cases, the PBP correction yields a sharper response compared to the true response of the column.

When the TIS correction procedure is applied, the corrected profile obtained, while being closer to the true response, yields spurious oscillations. This behaviour results as according to the TIS model, the inlet concentration profile should rise sharply similar to the true response of the column. However, in the formulation of the optimization problem in Eqn. 12, sharp changes in inlet concentration profile are penalized which gives rise to oscillations in the estimated $C_0(t)$.

While a theoretically sound method for elimination of the oscillations in the estimated inlet concentration profile is being currently researched, we present a simple heuristic based method to overcome this difficulty in the following discussion. From the previous examples, we note that during the adsorption process, $C_0(t)$ monotonically increases with time. In the presence of spurious oscillations, however, the gradient of $C_0(t)$ becomes negative at certain times. Thus, the oscillations in $C_0(t)$ can be removed by solving a constrained optimization problem with the objective function being given by Eqn. 12 and non-negativity constraints on $\Delta \widehat{\mathbf{C}}_0$, i.e.

$$\Delta \widehat{\mathbf{C}}_0(i) \geq 0; \quad i = 1, 2, \cdots, n_{\mathrm{samp}} \tag{17}$$

The corresponding constraint for a desorption experiment can be written as

14

$$\Delta \widehat{\mathbf{C}}_0(i) \leq 0; \quad i = 1, 2, \cdots, n_{\mathrm{samp}} \tag{18}$$

The resulting optimization problem can be easily cast a quadratic programming problem and can be solved using available mathematical tools, e.g. *quadprog* in the optimization toolbox of Matlab. As seen from Fig. 11, the introduction of the constraints dampens the oscillation resulting in more realistic breakthrough profiles. However, we do recognize that this method of formulating constraints will fail for systems exhibiting "roll-up" effects owing to competitive adsorption between components involved (Santacesaria et al., 1982).

7 Conclusion

The correction of breakthrough profiles for extra-column effects was studied. Traditionally, a point-by-point correction scheme has been used which implicitly assumes linear additivity of the retention time and band broadening. This paper highlights the potential pitfalls of this method. It has been shown that this procedure often results in a sharper breakthrough curve as compared the true response of the column leading to incorrect estimation of the mass transfer coefficients and equilibrium parameters. In cases where the exit flow rate changes as the breakthrough proceeds, the PBP scheme also leads to discrepancies in retention time. In some cases, it was also shown that the PBP can provide misleading information by masking characteristic mass transfer resistances.

In this paper we suggest that the extra-column effects be modeled as tanks-in-series, and further propose an inversion algorithm that is able to overcome the pitfalls of the PBP method This was demonstrated using a host of examples. It has been shown that the inversion of TIS model provides a more accurate method for correction of breakthrough profiles over a wider range of operating conditions as compared to the PBP scheme. An alternate approach will be to compare the composite responses from experiments and simulations, as opposed to comparing the true responses. This method, it might appear, can circumvent the correction of the composite response to obtain the true response. However, the importance of obtaining the true response are the following: Firstly, key information concerning underlying mass transfer mechanisms may be masked by the dynamics of the extra-column volume (note that in Fig. 8 the characteristic take-off, a signature of systems exhibiting barrier resistance, is smoothened out by the extra-column dynamics). Secondly, practitioners wishing to obtain equilibrium and kinetic parameters by fitting experimental results to analytical solutions of column dynamics equations, e.g. methods based on the calculation of moments, should base their analysis on

15

the true response rather than on the composite response. In conclusion, we
have identified regions where the PBP correction procedure leads to incorrect
prediction of the true response of the column, while the TIS model makes a
more accurate prediction. However, it should be mentioned that the choice of
the model to be used depends largely on the accuracy that the user intends
to achieve from the experiments.

8 Software

A free copy of the Matlab code used for the inversion of the TIS model can
be obtained by contacting the corresponding author.

9 Notation

b	Langmuir isotherm parameter
C	Gas phase concentration of adsorbable component
C_{T}	Total gas phase concentration
$\overline{C}$	Dimensionless gas phase concentration of adsorbable component
$\widehat{C}$	Deviation variable for concentration
D_{L}	Axial dispersion coefficient
G	Hankel matrix
k	LDF coefficient
K	Henry constant
L	Length of the adsorption column
n_{samp}	Number of samples
N	Number of tanks
q	Solid phase concentration of adsorbable component
q_{s}	Solid phase concentration at saturation of adsorbable component
$\overline{q}$	Dimensionless solid phase concentration of adsorbable component
q^*	Equilibrium solid phase concentration of adsorbable component
P	Pressure
Pe	Peclet number
Q	Volumetric flow rate
R_{g}	Universal gas constant
t	Time
T	Temperature
v	Velocity
$\overline{v}$	Dimensionless velocity
V_{dead}	Dead volume
z	Axial coordinate

Subscripts and Superscripts

in	Conditions at column inlet
out	Conditions at exit of the last tank
0	Conditions at column exit

Greek symbols

β	Ridge parameter
γ	Dimensionless LDF coefficient
θ	Dimensionless time
ϵ	Void fraction of the column
χ	Dimensionless length
λ	Langmuir non-linearity parameter
τ	Tank residence time in the TIS model
ψ	Dimensionless phase ratio

References

Atomic Energy Corporation of Canada. (1976). Forsim, a fortran package for the automated solution of coupled partial and/or ordinary differential equation systems.

Farooq, S., Qinglin, H., & Karimi, I. (2002). Identification of transport mechanism in adsorbent micropores from column dynamics. *Ind. Engg. Chem. Res.*, **41**(5), 1098–1106.

Gritti, F., Felinger, A., & Guiochon, G. (2006). Influence of the errors made in the measurement of the extra-column volume on the accuracies of estimates of the column efficiency and the mass transfer kinetics parameters. *J. Chromatogr. A*, **1136**(1), 57–72.

Guntuka, S. (2006). *Perovskite-based adsorption process for high temperature gas separation.* Masters Thesis, National University of Singapore.

Guntuka, S., Farooq, S., & Rajendran, A. (2007). A- and B- site substituted lanthanum cobaltite perovskite as high temperature oxygen sorbent 2. column dynamics study. *Ind. Engg. Chem. Res.*, accepted for publication.

Hansen, P. C. (1992). Analysis of ill-posed problems by means of the L-curve. *SIAM Review*, **34**, 561–580.

Hoerl, A. E. & Kennard, R. W. (1970). Ridge regression: Biassed estimation for nonorthogonal problems. *Technometrics*, **12**, 55–67.

Levenspiel, O. (1998). *Chemical Reaction Engineering.* John Wiley and Sons, New York, 3rd edition.

Malek, A., Farooq, S., Rathor, M., & Hidajat, K. (1995). Effect of velocity variation due to adsorption-desorption on equilibrium data from breakthrough experiments. *Chem. Eng. Sci.*, **50**(4), 737–740.

Ruthven, D. (2000). Past progress and future challenges in adsorption research. *Ind. Engg. Chem. Res.*, **39**, 2127–2131.

Ruthven, D. M. (1984). *Principles of adsorption and adsorption processes.* John Wiley, New York.

Ruthven, D. M., Farooq, S., & Knaebel, K. S. (1994). *Pressure swing adsorption.* VCH Publishers, New York.

Santacesaria, E., Morbidelli, M., Servida, A., Storti, G., & Carra, S. (1982). Separation of xylenes on Y zeolites. 2. Breakthrough curves and their interpretation. *Ind. Engg. Chem. Process Design Develop.*, **21**, 446–451.

Seborg, D. E., Edgar, T. F., & Mellichamp, D. A. (2003). *Process dynamics and control.* John Wiley and Sons, Hoboken, NJ.

Shankar, A. & Lenhoff, A. (1991). Dispersion in round tubes and its implications for extracolumn dispersion. *J. Chromatogr.*, **556**(1-2), 235–248.

Sircar, S. (2002). Pressure swing adsorption. *Ind. Engg. Chem. Res.*, **41**(6), 1389–1392.

Sircar, S. (2007). Recent developments in macroscopic measurement of multicomponent gas adsorption equilibria, kinetics, and heats. *Ind. Engg. Chem. Res.*, **46**(10), 2917–2927.

Tikhonov, A. N. (1963). Solution of incorrectly formulated problems and the regularization method. *Soviet Math Dokl*, **4**, 1035–1038.

Yang, R. T. (1987). *Gas separation by adsorption processes.* Imperial College Press, London.

Legend: (○)- True response of the column, C_0/C_{in}; (◆) - Composite response, C_{out}/C_{in}; (◇) - Blank response; (– –) Corrected response using PBP, (—) - Corrected response using TIS model C_0/C_{in}; (—△—) - Dimensionless flow rate, Q_0/Q_{in}. (a) number of tanks, $N = 5$, (b) number of tanks, $N = 20$. See Table 2 for parameters.

Figure 9:
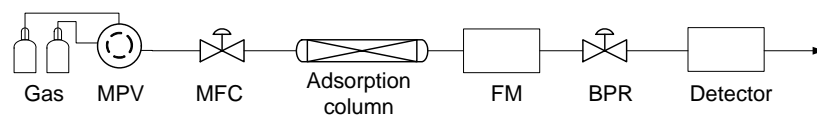Comparison of PBP and TIS inversion techniques corresponding to Case 3. Legend: (○)- True response of the column; (◆) - Composite response; (◇) - Blank response; (– –) Corrected response using PBP, (—) - Corrected response using TIS model; (—△—) - Dimensionless flow rate. (a) number of tanks, $N = 5$, (b) number of tanks, $N = 20$, see Table 2 for parameters.

Figure 10:
Comparison of PBP and TIS inversion techniques corresponding to Case 4. Legend: (○)- True response of the column, C_0/C_{in}; (◆) - Composite response, C_{out}/C_{in}; (◇) - Blank response; (– –) Corrected response using PBP, (—) - Corrected response using TIS model C_0/C_{in}; (—△—) - Dimensionless flow rate, Q_0/Q_{in}. (a) number of tanks, $N = 5$, (b) number of tanks, $N = 20$. See Table 2 for parameters.

Figure 11:
Comparison of PBP and TIS inversion techniques corresponding to Case 5. The true and the corrected responses are shown in the main figure while the composite and blank responses are shown in the inset. Legend: (○)- True response of the column, C_0/C_{in}; (◆) - Composite response, C_{out}/C_{in}; (◇) - Blank response. (a) number of tanks, $N = 5$, (b) number of tanks, $N = 20$, see Table 2 for parameters.

List of Table Captions

21

(a) Composite response

(b) Blank response

MPV- Multi-position switch valve   FM – Flow meter
MFC- Mass flow controller   BPR- Back pressure regulator
ZDV – Zero-dead-volume

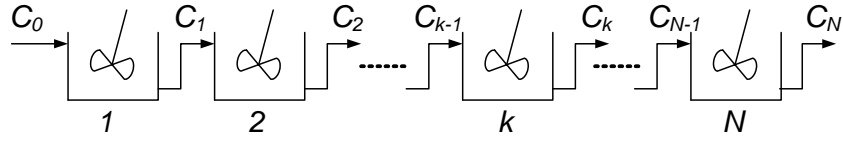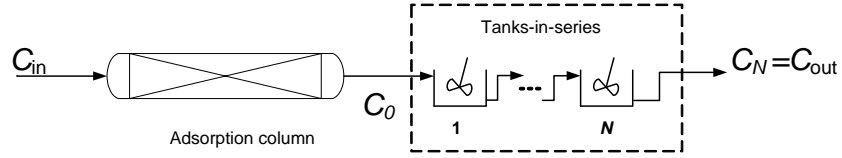Fig. 1. Simplified schematic for various experiments performed to correct for extra–column contributions.
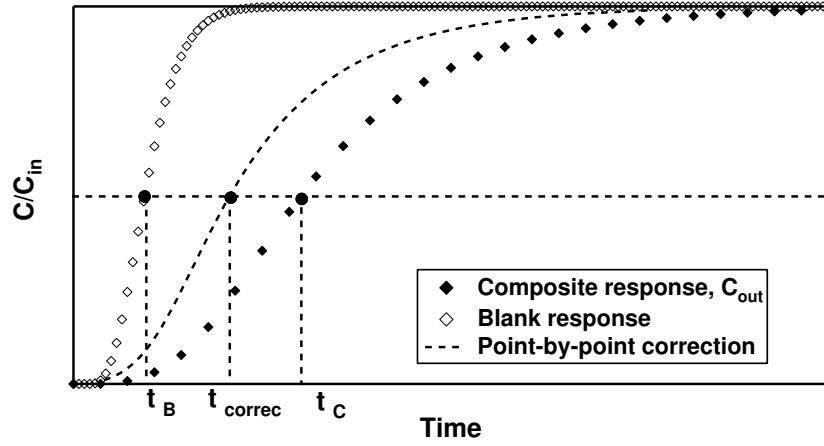
Fig. 2. Qualitative responses for experimental configurations shown in Fig. 1 and illustration of the point by point correction procedure.

(a) Schematic of Tanks-in-series (TIS) model

(b) Modeling dispersion in extra-column volume

Fig. 3. Schematic of the tanks-in-series (TIS) model for description of extra-column effects.
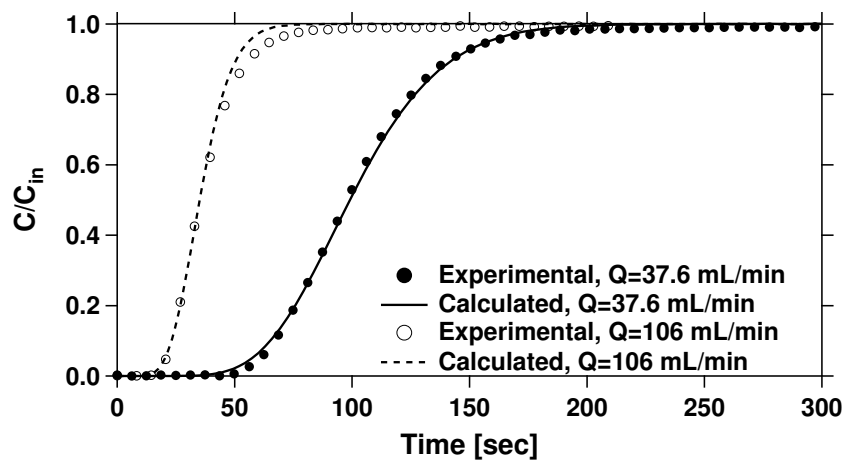
Fig. 4. Experimental (symbols) responses of direct injection into the detector. Fitted volume = 64 mL, number of tanks, N=11. Lines depict the fitted response using a tanks-in-series model.
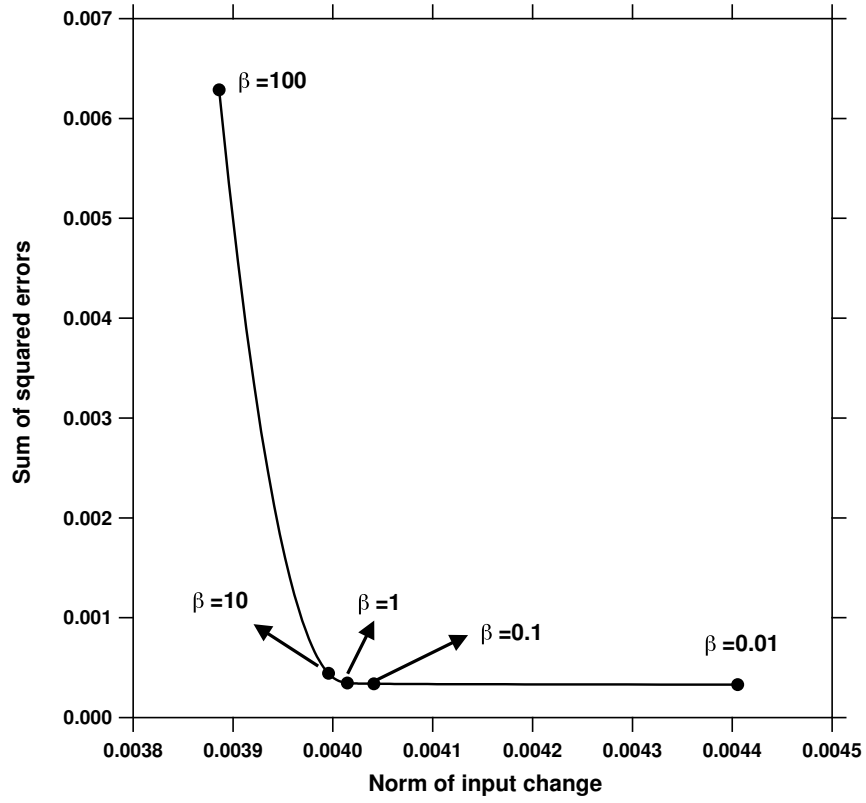
Fig. 5. Plot of sum of squared errors as a function of the norm of input change for example shown in Fig. 6 (a).
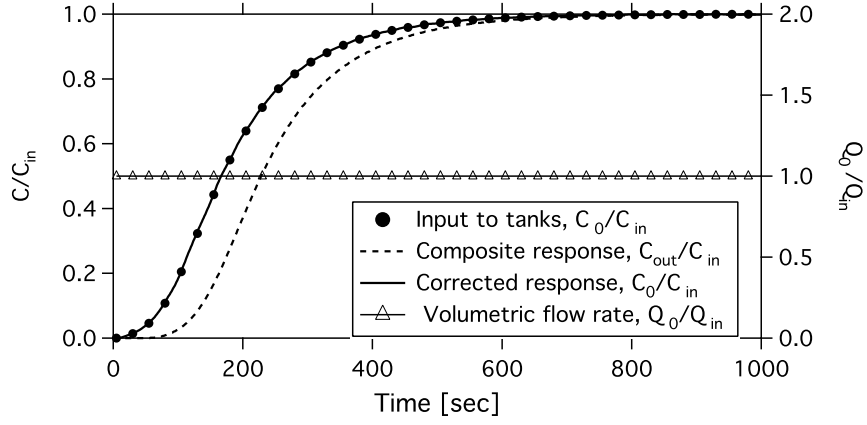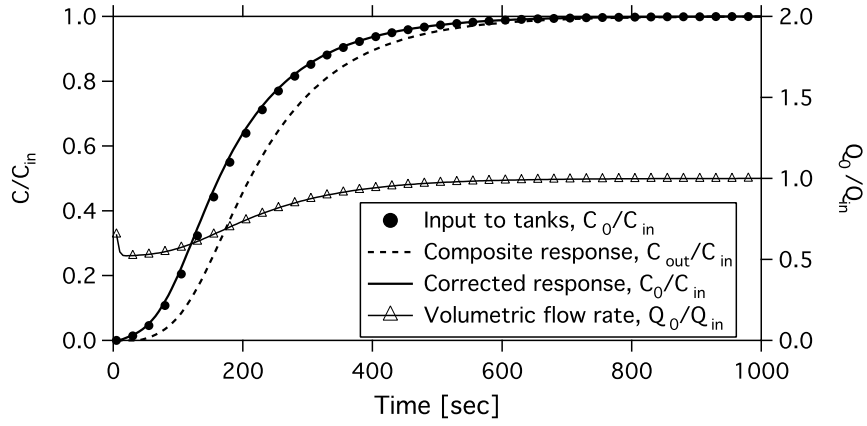
Fig. 6. Inversion of the TIS model for (a) no variation of inlet flowrate and (b) with variation inlet flowrate.
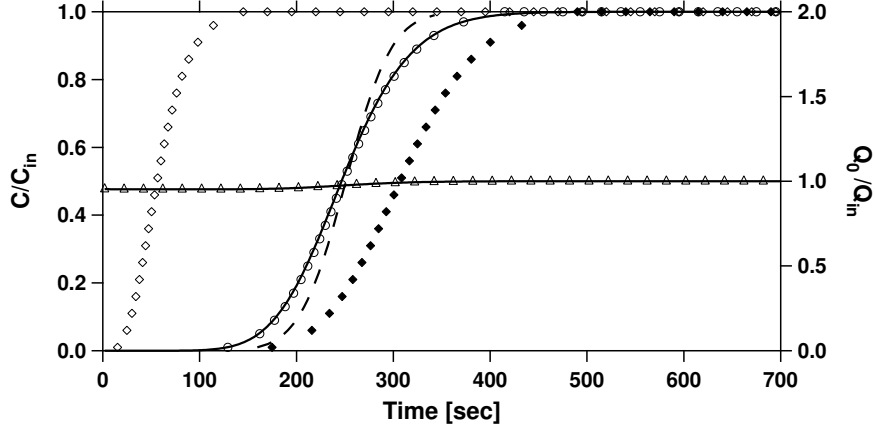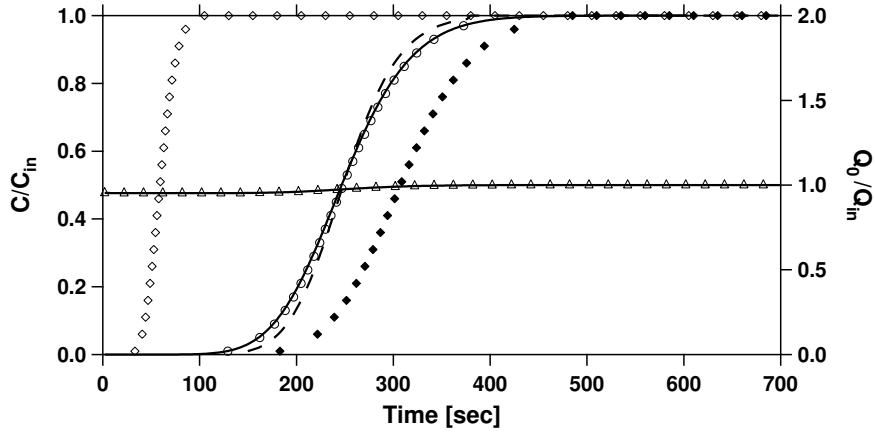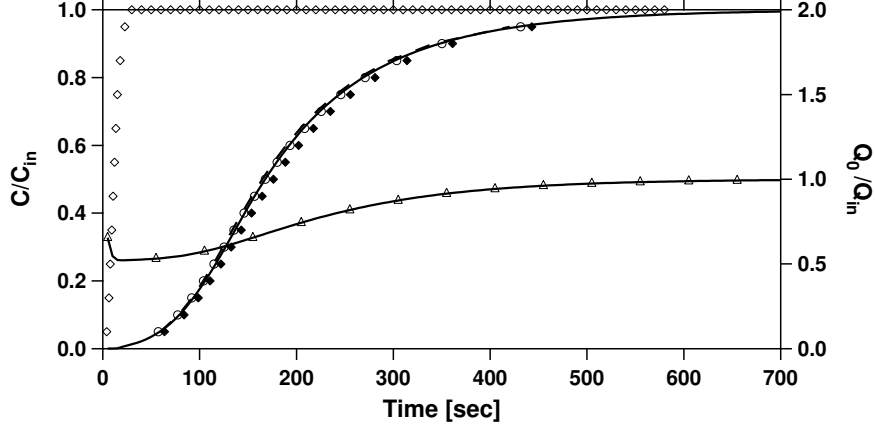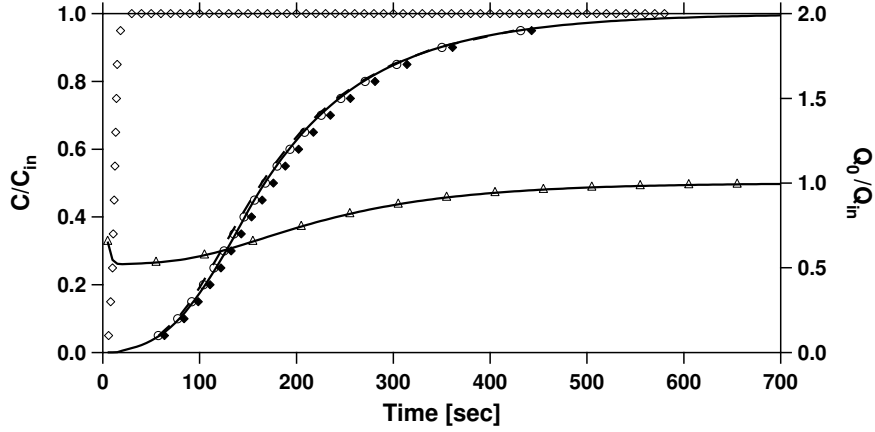
Fig. 7. Comparison of PBP and TIS inversion techniques corresponding to Case 1. Legend: (○)- True response of the column, C_0/C_{in}; (♦) - Composite response, C_{out}/C_{in}; (◇) - Blank response; (– –) Corrected response using PBP, (—) - Corrected response using TIS model C_0/C_{in}; (—△—) - Dimensionless flow rate, Q_0/Q_{in}. (a) number of tanks, $N = 5$, (b) number of tanks, $N = 20$. See Table 2 for parameters.
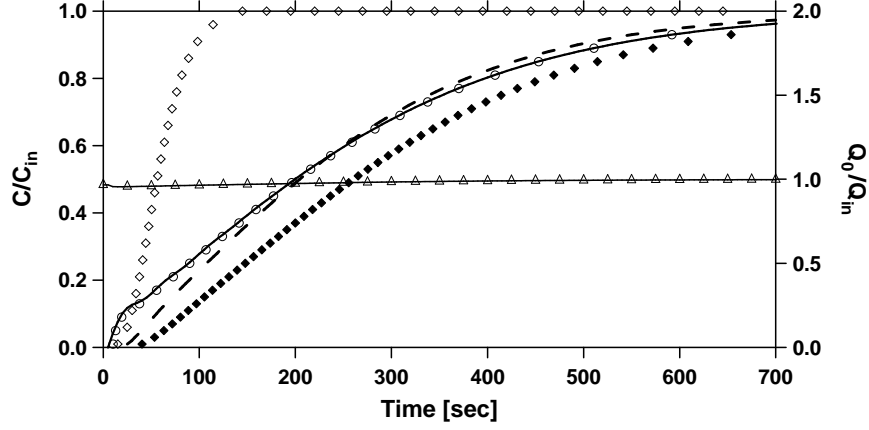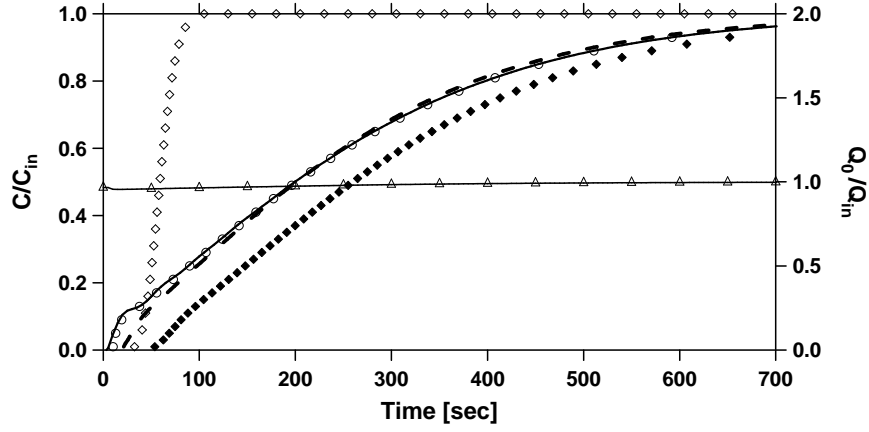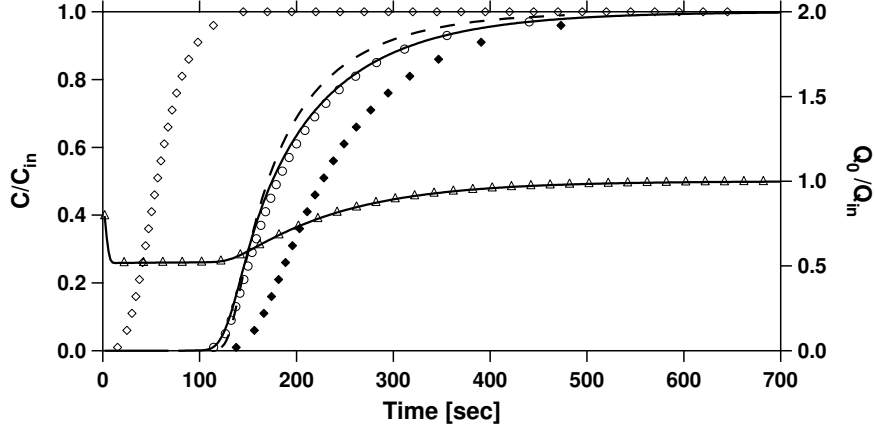
Fig. 8. Comparison of PBP and TIS inversion techniques corresponding to the Case 2. Legend: ($\circ$)- True response of the column, C_0/C_{in}; ($\blacklozenge$) - Composite response, $C_{\text{out}}/C_{\text{in}}$; ($\diamondsuit$) - Blank response; ($--$) Corrected response using PBP, ($-$) - Corrected response using TIS model C_0/C_{in}; ($-\triangle-$) - Dimensionless flow rate, Q_0/Q_{in}. (a) number of tanks, $N = 5$, (b) number of tanks, $N = 20$. See Table 2 for parameters.
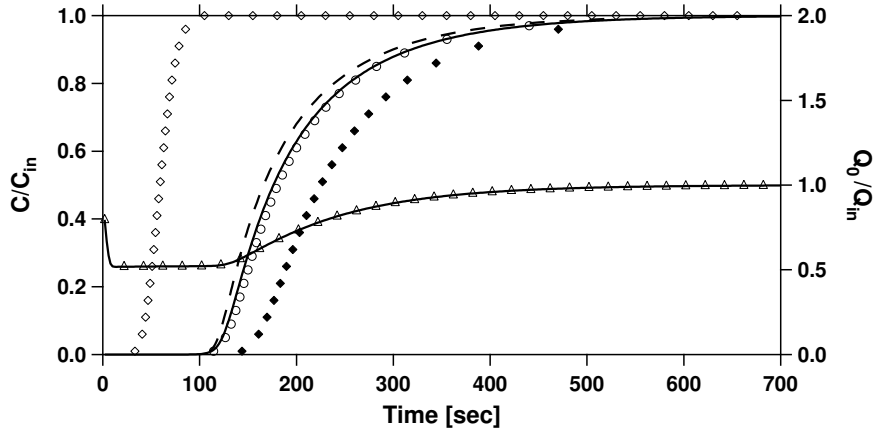
Fig. 9. Comparison of PBP and TIS inversion techniques corresponding to Case 3. Legend: (○)- True response of the column, C_0/C_{in}; (♦) - Composite response, C_{out}/C_{in}; (◇) - Blank response; (– –) Corrected response using PBP, (—) - Corrected response using TIS model C_0/C_{in}; (—△—) - Dimensionless flow rate, Q_0/Q_{in}. (a) number of tanks, $N = 5$, (b) number of tanks, $N = 20$. See Table 2 for parameters.
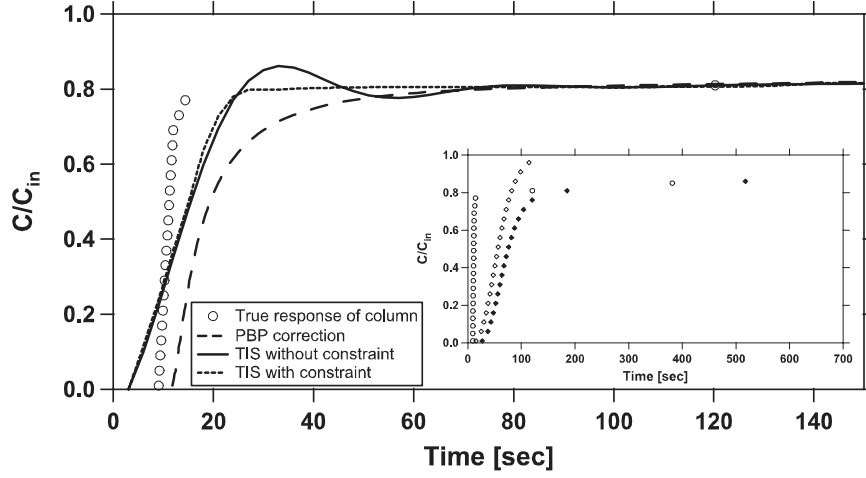
Fig. 10. Comparison of PBP and TIS inversion techniques corresponding to Case 4. Legend: (○)- True response of the column, C_0/C_{in}; (◆) - Composite response, C_{out}/C_{in}; (◇) - Blank response; (– –) Corrected response using PBP, (—) - Corrected response using TIS model C_0/C_{in}; (—△—) - Dimensionless flow rate, Q_0/Q_{in}. (a) number of tanks, $N = 5$, (b) number of tanks, $N = 20$. See Table 2 for parameters.

31

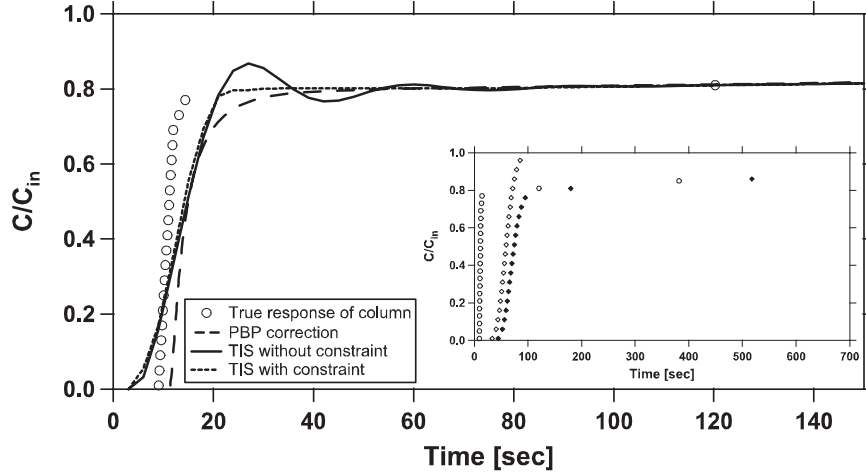Fig. 11. Comparison of PBP and TIS inversion techniques corresponding to Case 5. The true and the corrected responses are shown in the main figure while the composite and blank responses are shown in the inset. Legend: (○)- True response of the column, C_0/C_{in}; (◆) - Composite response, C_{out}/C_{in}; (◇) - Blank response. (a) number of tanks, $N = 5$, (b) number of tanks, $N = 20$, see Table 2 for parameters.

Parameter	Value
Column length, L [cm]	35.00
Bed voidage of the column, ϵ	0.40
Pressure, P [atm]	1.00
Temperature, T [$^\circ$C]	25.00
Henry constant, K	14.80
Solid saturation capacity, q_s [$\times 10^{-3}$ mol /mL]	5.26
Molecular diffusivity, D_m [cm^2/s]	0.20

Table 1
Parameters for simulation.

Parameter	Case 1	Case 2	Case 3	Case 4	Case 5
LDF coefficient, k [1/s]	0.100	0.010	0.010	0.010	0.001
Non-linearity parameter, λ	0.10	0.50	0.50	0.90	0.10
Inlet volumetric flow rate, Q_{in} [mL/s]	1.00	1.00	5.00	1.00	1.00
Inlet gas phase mole fraction , X_{in}	0.05	0.05	0.50	0.50	0.05

Table 2

Parameters for case study.